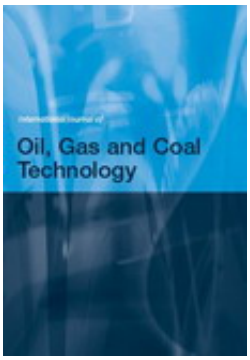

International Journal of Oil, Gas and Coal Technology

ISSN online: 1753-3317 - ISSN print: 1753-3309
https://www.inderscience.com/ijogct

Study on the law of disaster caused by multi-field coupling of coal and gas near fault tectonic zone

Chong Liu, Zhifan Lu, Zhiyu Dong, Kaiwen Ren, Jie Ma, Junfeng Wang

DOI: 10.1504/IJOGCT.2025.10073161

Article History:

Received:	25 December 2024
Last revised:	24 June 2025
Accepted:	05 August 2025
Published online:	04 November 2025

Study on the law of disaster caused by multi-field coupling of coal and gas near fault tectonic zone

Chong Liu

College of Mining Engineering,
Taiyuan University of Technology,
Taiyuan, 030024, China
and
Shanxi Xinyuan Coal Limited Liability Company,
Jinzhong, 046000, China
Email: liuchong.871010@163.com

Zhifan Lu, Zhiyu Dong, Kaiwen Ren, Jie Ma and Junfeng Wang*

College of Mining Engineering,
Taiyuan University of Technology,
Taiyuan, 030024, China
Email: 17277053791@163.com
Email: 941015@163.com
Email: 13303545425@163.com
Email: m87194582@163.com
Email: wangjunfeng@tyut.edu.cn
*Corresponding author

Abstract: To explore the multi-field coupling disaster-causing laws near fault tectonic, the multi-physical field evolution characteristics of conventional coal seams and the fault-containing coal seams were compared and analysed, and the energy change laws during the mining process of fault-containing coal seams were investigated. The findings reveal that compared to conventional coal seams, stress concentration and gas accumulation inside fault-containing coal seams were more significant. Elastic energy and gas expansion energy dominate the evolution of the outburst process. Elastic strain can lead to an increase in gas expansion energy within the coal seam. The proportion of free gas expansion energy in the total energy is relatively small, and its contribution to gas outburst is also relatively small. The key to gas outburst lies in the instantaneous release of a large amount of adsorbed gas expansion energy. The research findings are important for understanding the multi-field coupling disaster mechanism near fault tectonic. [Received: January 4, 2025; Accepted: August 5, 2025]

Keywords: gas outburst; multi-field coupling; fault tectonics; permeability.

Reference to this paper should be made as follows: Liu,C., Lu, Z., Dong, Z., Ren, K., Ma, J. and Wang, J. (2025) 'Study on the law of disaster caused by multi-field coupling of coal and gas near fault tectonic zone', *Int. J. Oil, Gas and Coal Technology*, Vol. 38, No. 5, pp.1–23.

Biographical notes: Chong Liu is a Senior Engineer, mainly engaged in technical research in coal mine gas prevention and control, gas geology and other aspects.

Zhifan Lu is a Doctoral student, mainly engaged in research in the field of intelligent early warning and prevention and control of coal mine disasters.

Zhiyu Dong is a Doctoral student, mainly engaged in the research of coal spontaneous combustion mechanism and its prevention and control.

Kaiwen Ren is a Doctoral student, mainly engaged in the research of coal spontaneous combustion mechanism and its prevention and control.

Jie Ma is a graduate student, mainly engaged in research in the field of intelligent early warning and prevention and control of coal mine disasters.

Junfeng Wang is a famous expert in mine disaster prevention, specialising in coal and gas outburst dynamics and control technologies. With rich field experience and academic achievements, he has many led key researches, published influential papers, and developed applied safety technologies, boosting mine disaster mitigation globally.

1 Introduction

Coal and gas outburst are common dynamic disasters during coal mining. China's shallow coal resources have been depleted by years of large-scale, continuous mining, necessitating gradual advancement of coal mining activities to deeper parts of the stratum (Wang et al., 2023a). However, the high-temperature and high-pressure environment of such deep coal mines exacerbates the difficulty of controlling kinetic disasters (Zhao, 2021; Xie et al., 2023). Although outburst occurrences and fatalities in Chinese coal mines have exhibited decreasing trends in recent years (Cao, 2024), the proportion of fatalities caused by outburst to the total number of fatalities in coal mines has generally risen (Fan et al., 2024). At this stage, coal mining safety remains precarious, and the prediction and prevention of coal and gas outbursts have a long way to go (Jia et al., 2023).

Production practice and data have proved that the number of coal and gas outbursts in fault tectonic areas is much higher than that in other areas (Cao et al., 2022). Therefore, exploring the dynamic mechanism of coal and gas outbursts in fault tectonic zones is urgently needed. The geological structure affects the strength of the coal body, gas storage characteristics, and formation of tectonic coal areas (Cheng and Wang, 2024). Liu et al. (2024a) compared and analysed the mechanical and destructive characteristics of primary coal and tectonic coal with the help of uniaxial experiment and found that tectonic coal is more prone to deformation and destruction under the same stress conditions, which indicates that tectonic coal has a high risk of gas outburst. Wang and Cheng (2017) conducted an experimental study on the pore characteristics and gas desorption law of tectonic coal and primary coal, and found that geological tectonics has an obvious modification effect on the medium and large pores of the coal, but the micropores and small pores are the main adsorption space for gas. Tectonic action affects the desorption performance of coal by modifying the pore structure of coal. Meng et al.

(2022) studied the difference of methane diffusion performance between tectonic coal and primary coal, and found that the diffusion coefficients of both primary and tectonic coal decreased with the decrease of pressure, but the diffusion coefficients of tectonic coal were higher than that of primary coal in the whole diffusion stage. Cheng and Lei (2021) conducted an in-depth study on the intrinsic relationship between tectonic coal and gas outburst, and found that compared with primary coal, tectonic coal has larger pore volume and specific surface area, and its adsorption/desorption coefficients are larger, but its mechanical strength is weaker, and the above characteristics make it prone to gas outburst. The above analysis shows that the mechanical strength and adsorption characteristics of tectonic coal are different from those of primary coal, which leads to differences in the risk of gas outburst in different areas of mines, but there are fewer studies on how fault tectonics lead to coal and gas outburst.

Coal and gas dynamic disaster is a complex process involving multi-physical field coupling of coal and rock deformation and gas transport, but the current experimental research mostly analyses the influence of fault structure on coal and gas outburst from a single perspective, and the multi-physical field coupling disaster-causing law of coal and gas in the process of fault-containing coal seam mining has not yet been clarified. Guo et al. (2023) analysed the stress field distribution characteristics of the mine structure through on-site measurements, and found that the evolutionary effect of multi-phase tectonic stress field caused the regional distribution of tectonic coal, geostress, and coal seam gas. And the horizontal extrusion stress of the tectonic stress field would cause a gas outburst disaster mainly of the press-out type. Gao et al. (2021) investigated the effect of blasting disturbance on coal and gas disasters in the fault area, and found that the propagation and reflection of blasting stress waves in the fault area exacerbated the stress concentration and energy accumulation within the fault area, which provided the basis for the occurrence of coal and gas outburst. Song and Wei (2017) studied the gas distribution characteristics near small fault, and found that the cracks in the fault area were fully developed, but the permeability of the fault surface was poor, which provided good conditions for gas enrichment. Chen et al. (2019) analysed the coalbed methane (CBM) storage characteristics at different burial depths and geological formations via sampling, reporting that CBM content increased with burial depth, and the CBM content near faults was 1.6 times higher than that in normal areas.

In this study, a multi-physical field coupling model describing the mutual coupling of stress field, seepage field, coal matrix and coal fissure gas transport in the coal seam mining process was constructed based on the dual porosity characteristics of coal, taking the Lu'an Group Xinyuan Mine as the geological background. A comparative analysis of the evolution law of each physical field in the coal seam after the exposure of the working face of conventional and fault-containing coal seams was carried out firstly. Then the evolution characteristics and energy change law of each physical field during the working face close to the fault zone were studied in depth. The results of the study contribute to the in-depth understanding of the coal and gas outburst mechanism in fault tectonic zones.

2 Mathematical model of multi-physical field coupling between coal and gas

2.1 Model assumptions

Coal is characterised by a dual pore structure (Zhao et al., 2020), as shown in Figure 1. The coal body consists of two parts, the matrix and fracture, where L_m and L_f are the widths of the unit coal matrix and fracture, respectively. In addition, smaller pores exist within the coal matrix. The coal matrix structure is deformed under the actions of stress and gas pressure. The numerical model developed herein is capable of describing the multi-physical field coupling of coal and gas during mining under the following assumptions:

1 coal and rock bodies are isotropic porous media consisting of skeleton, matrix pores and fracture

2 both the coal and the rock seam undergo elastic deformation under external force, and their deformation is consistent with the small deformation hypothesis

3 the mechanical strength of both coal and rock inside the fault is weaker than in the area outside the fault

4 the adsorption and desorption effects of gas in coal and rock seam are consistent with the extended Langmuir equation

5 diffusion of gases in both coal matrix and rock follows Fick's law, and seepage follows Darcy's law.

Figure 1 Dual porosity model of coal (see online version for colours)

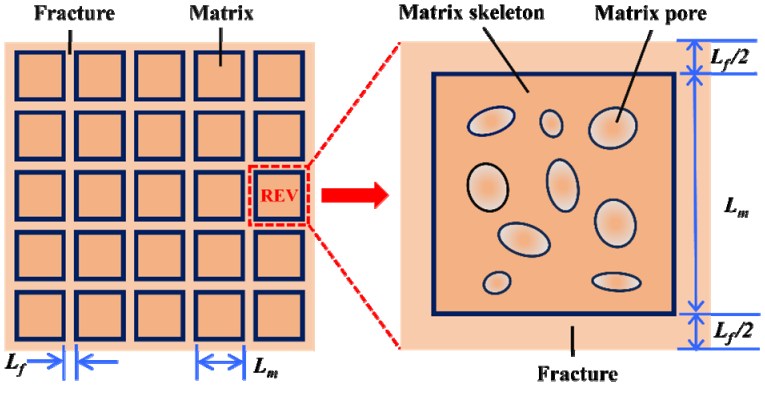

2.2 Controlling equations of gas transport in coal matrix

The gas in the coal matrix mainly consists of two parts, the adsorbed state gas on the coal matrix and the free state gas inside the matrix pores (Liu et al., 2024a), which can be expressed as:

$$m_m = \frac{abp_m\rho_c M}{\left(1+bp_m\right)V_m} + \phi_m \frac{Mp_m}{RT} \tag{1}$$

where m_m is the mass per unit of coal, a is Langmuir volume constant, b is Langmuir pressure constant, p_m is the gas pressure in the coal matrix, V_m is the molar volume of the gas, ρ_c is the density of the coal, M is the molar mass of the gas, Φ_m is the porosity of the coal matrix, R is the molar gas constant, and T is the ambient temperature of the coal.

The mass exchange between the coal matrix and the coal fracture can be expressed as (Mora and Wattenbarger, 2009):

$$Q_s = \frac{3\pi^2 M\left(p_m - p_f\right)D_0 \exp(-\lambda t)}{{L_m}^2 RT} \tag{2}$$

where Q_s is the mass source, p_f is the fracture pressure, D_0 is the initial gas diffusion coefficient, λ is the attenuation coefficient, and t is time, T is the coal temperature.

The transport of gas in the coal matrix conforms to Fick's law of diffusion and can be expressed as (Liu et al., 2015):

$$\frac{\partial m_m}{\partial t} = -Q_s = -\frac{3\pi^2 M\left(p_m - p_f\right)D_0 \exp(-\lambda t)}{{L_m}^2 RT} \tag{3}$$

2.3 Controlling equations for gas transport in coal fracture

The transport of gas in coal fractures is mainly seepage, and according to the law of mass conservation, the process can be expressed as (Zhao et al., 2019):

$$\frac{\partial}{\partial t}\left(\phi_f \rho_f\right) + \nabla\left(\rho_f V_f\right) = \left(1-\phi_f\right)Q_s \tag{4}$$

where ϕ_f is the porosity of the coal fissure; ρ_f is the gas density inside the coal fracture, $\rho_f = \frac{M}{RT}p_f$; p_f is the gas pressure inside the coal fracture; and V_f is the seepage velocity of the coal fracture gas, $V_f = -\frac{k_f}{\mu}\nabla p_f$; k_f is the permeability of the coal fracture; and μ is the kinetic viscosity of the gas.

Bringing equation (2) into equation (4), the gas seepage equation within the coal fractures can be obtained as.

$$\phi_f \frac{\partial p_f}{\partial t} + p_f \frac{\partial \phi_f}{\partial t} + \nabla\left[-\frac{k_f}{\mu}p_f \nabla p_f\right] = \frac{3\pi^2 D_0\left(1-\phi_f\right)\exp(-\lambda t)}{{L_m}^2}\left(p_m - p_f\right) \tag{5}$$

2.4 Controlling equations for coal seam deformation

Considering the effects of gas diffusion in the coal matrix and gas migration in the coal fracture on the coal deformation, the stress change of coal seam with dual pore structure can be expressed as (Li et al., 2023):

$$Gu_{i,jj} + \frac{G}{1-2v}u_{j,ji} - \left(\alpha_m p_{m,i} + \alpha_f p_{f,i}\right) - K\varepsilon_{s,i} + f_i = 0 \tag{6}$$

where

$$G = \frac{E}{2(1+v)}, K = \frac{E}{3(1-2v)}, \alpha_m = 1 - \frac{K}{K_m}, \alpha_f = 1 - \frac{K}{K_f},$$
$$K_m = \frac{E_m}{3(1-2v)}, \varepsilon_s = \frac{\varepsilon_L p_m}{p_m + p_L},$$

G is the shear modulus of coal, K is the bulk modulus of coal, E is the modulus of elasticity of coal, v is the Poisson's ratio, α_m and α_f are the Biot coefficients for coal matrix and coal fracture, respectively, ε_s is the adsorptive strain of coal, p_m is the gas pressure within the coal matrix, and p_f is the gas pressure within the coal fracture, p_L is the Langmuir pressure constant, ε_L is the Langmuir bulk strain constant, E_m is the elastic modulus of the coal skeleton, K_m is the bulk modulus of the coal matrix, and K_f is the fracture bulk modulus.

The numerical simulation process considers the coal seam as an isotropic continuous deformation medium, and the relationship between strain and stress can be expressed as (Zhang et al., 2008):

$$\begin{cases} \sigma_{ij,i} + f_j = 0 \\ \varepsilon_{ij} = \dfrac{1}{2}\left(u_{i,j} + u_{j,i}\right) \end{cases} \tag{7}$$

where f_j is the coal force, $u_i (i = x, y, z)$ is the displacement of coal in the direction of i.

2.5 Controlling equations for coal damage evolution

Coal seam will be damaged and destroyed under the action of mining disturbance stress and gas pressure. Based on the damage theory (Zheng et al., 2018a), the elastic modulus of the coal body will change as shown in Figure 2. In the elastic stage, the elastic modulus of the coal body stays unchanged and the coal body will not be damaged. And when the stress carried by the coal body reaches the peak value, the coal body will be damaged and destroyed.

The elastic modulus of the coal body in this process can be expressed as:

$$E = E_0(1 - D) \tag{7}$$

where E and E_0 are the elastic modulus of the coal after and before damage, respectively; D is the damage variable.

The tensile and shear damage that occurs after the coal body is stressed is determined in the simulation by the maximum tensile stress criterion and the Mohr Coulomb criterion, and the process can be expressed as follows (Zheng et al., 2018b):

$$F_1 = \sigma_1 - \sigma_t = 0$$
$$F_2 = -\sigma_3 + \sigma_1 \frac{1+\sin\theta}{1-\sin\theta} - \sigma_c = 0 \tag{8}$$

where, σ_1 and σ_3 are the maximum and minimum principal stress, respectively; σ_t and σ_c are the uniaxial tensile and uniaxial compressive strength of the coal, respectively; θ is the angle of internal friction of the coal; F_1 and F_3 are the threshold functions for tensile and shear damage, respectively.

Figure 2 Elastic damage evolution model of coal

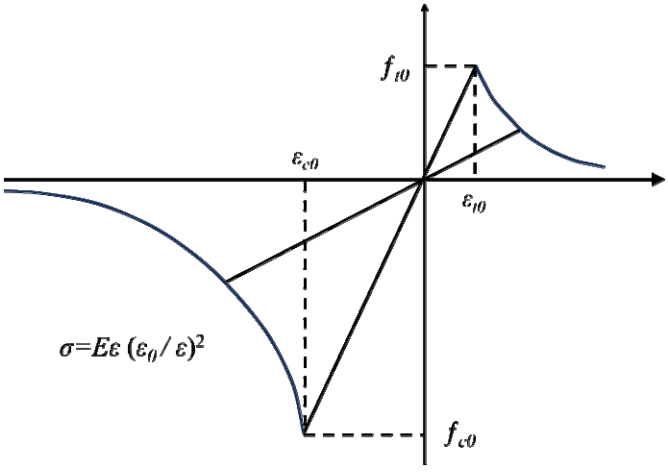

The relationship between damage and strain generated in the coal seam under the effect of mining disturbance can be expressed as (Fan et al., 2017):

$$D=\begin{cases}0 & F_1<0, F_2<0\\ 1-\left|\dfrac{\varepsilon_{t0}}{\varepsilon_1}\right|^2 & F_1=0, dF_1>0\\ 1-\left|\dfrac{\varepsilon_{c0}}{\varepsilon_3}\right|^2 & F_2=0, dF_2>0\end{cases} \tag{9}$$

where ε_1 is the maximum principal strain of coal; ε_3 is the minimum principal strain of coal; ε_{t0} is the ultimate tensile strain of coal when tensile damage occurs; ε_{c0} is the ultimate compressive strain of coal when shear damage occurs.

2.6 Controlling equations for coal seam porosity and permeability

Under the influence of mining activities, the stress state of the coal seam will be changed (Luo et al., 2023), which will lead to changes in the porosity and permeability of the coal seam, thus affecting the diffusion and migration of gas in the coal seam, and also the change of gas pressure affects the stress distribution of the coal seam (Li and Zhang, 2022). According to et al. the change in porosity of coal matrix can be expressed as (Liu et al., 2017):

$$\phi_m=\phi_{m0}e^{\frac{KK_m-K_mK_p+K_pK}{K_p(K_m-K)}\left\{\frac{K_mL_f}{K_fL_m+K_mL_f}\frac{p_L\varepsilon_L(p_m-p_{m0})}{(p_m+p_L)(p_{m0}+p_L)}+\frac{K_f(L_m+L_f)}{K_fL_m+K_mL_f}\varepsilon_V\right\}} \tag{10}$$

The change in porosity of coal fractures can be expressed as (Qu et al., 2018):

$$\frac{\phi_f}{\phi_{f0}} = 1 - \frac{K_m}{K_f L_m + K_m L_f}\left[\frac{p_L L_m \varepsilon_L (p_m - p_{m0})}{(p_m + p_L)(p_{m0} + p_L)} - (L_m + L_f)\varepsilon_V\right] \tag{11}$$

There is a cube relationship between porosity and permeability, therefore, the permeability of a coal fracture can be expressed as (Fu et al., 2022):

$$\frac{k_f}{k_{f0}} = \left(1 - \frac{K_m}{K_f L_m + K_m L_f}\left[\frac{p_L L_m \varepsilon_L (p_m - p_{m0})}{(p_m + p_L)(p_{m0} + p_L)} - (L_m + L_f)\varepsilon_V\right]\right)^3 \tag{12}$$

where ϕ_{m0} is the initial matrix porosity; p_{m0} is the initial matrix gas pressure; ϕ_{f0} is the initial fracture porosity; k_{f0} is the initial fracture permeability; ε_V is the coal volumetric strain.

3 Numerical modelling process

3.1 Physical modelling

The Xinyuan Mine of the Lu'an Group is a high-gas mine located at the northwest end of the Qinshui block depression area, and numerous fault zones have developed within the well field, which threatens safety during production of the coal mine. A physical model for the numerical simulations was constructed using working face 3410 of the Xinyuan Mine as the engineering background, as shown in Figure 3. The model size was 50 × 25 m, and the height of the coal seam was set at 5 m. In addition, a conventional coal seam model without a fault was established to comparatively analyse the influence of fault tectonics on coal and gas outbursts.

Figure 3 Physical models, (a) the fault-containing (b) the conventional coal seams (see online version for colours)

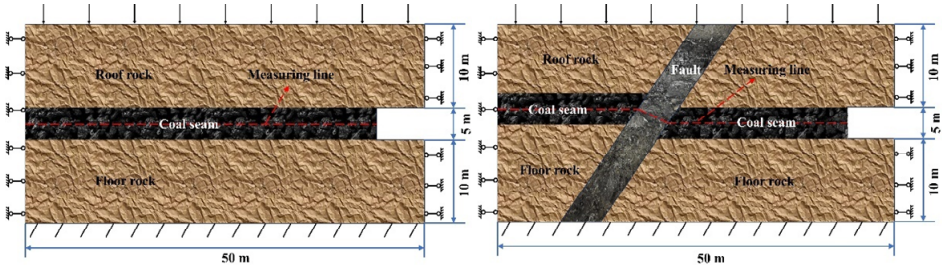

(a) (b)

3.2 Boundary condition settings

The stress boundary conditions in the model were set as follows: the bottom of the model was set as a fixed constraint, and the left and right sides were set as roll-supported boundaries, i.e., no lateral displacement occurred. Considering the depth of the coal seam,

a fixed load was selected at the top of the model, which was calculated according to the following formula (Peng et al., 2019):

$$\sigma = \gamma H \tag{13}$$

where σ is the original rock stress, MPa; γ is the self-weight of the overlying coal rock layer, and 2 t/m^3 is taken for this coal seam; H is the depth of the coal seam, and H = 500 m. According to equation (13), the applied stress in the top of the coal seam can be obtained as 10 MPa.

The boundary conditions of the seepage field were set as follows: the gas pressure of the exposed coal wall in the front of the working face was set to 0.1 MPa, i.e., one atmosphere; the initial gas pressure of the coal seam was 2 MPa; and the remaining boundaries were set as zero flux boundaries, i.e., gas flow was prohibited. According to the measured and experimental data in the mine, the specific parameters for the model are listed in Table 1.

Table 1 Specific parameters needed in the simulation

Parameter	*Value*	*Parameter*	*Value*
Langmuir volume constant, a	0.048 m^3/kg	Attenuation coefficient, λ	2×10^{-7}
Langmuir pressure constant, b	1 MPa^{-1}	Apparent density of coal, ρ_c	1,250 kg/m^3
Initial gas diffusion coefficient, D_0	3×10^{-11} m^2/s	Langmuir volume strain constant, ε_L	0.01266
Volume modulus of fracture, K_f	0.048 GPa	Elastic modulus of coal skeleton, E_m	8.469 GPa

Table 1 Specific parameters needed in the simulation (continued)

Parameter	*Value*	*Parameter*	*Value*
Gas constant, R	8.314 J/(mol·K)	Elastic modulus of coal, E	2.7 GPa
Poisson's ratio, ν	0.339	Elastic modulus of rock, E_r	20 GPa
Matrix width, L_m	0.001 m	Elastic modulus of fault, E_f	1.2 GPa
Fracture width, L_f	5×10^{-6} m	Initial fracture porosity, ϕ_f	0.001
Molar volume of gas, V_L	0.016 kg/mol	Initial matrix porosity, ϕ_{m0}	0.05
Molar mass of gas, M_C	0.016 kg/mol	Initial porosity of fault, ϕ_{ff}	0.064
Temperature, T	293.15 K	Initial fracture permeability, k_{f0}	1×10^{-15} m^2
Internal friction angle, φ	32 deg	Initial permeability of fault, k_{ff0}	1×10^{-13} m^2

4 Simulation results

4.1 Analysis of multi-physical field coupling in conventional coal seams

Figure 4(a) presents the stress distribution characteristics during mining of a conventional coal seam. The stress distribution in the area far away from the working face is basically unchanged during mining of the conventional coal seam, whereas that in the area leaning toward the working face is complicated. Specifically, the stress within the coal seam appears to first increase and then decrease closer to the working face, which was verified

by the stress distribution on the horizontal monitoring line of the coal seam in Figure 5(a). According to the above characteristics, stress changes within the coal seam can be divided into three zones:

1 In the area far away from the working face, the influence of mining activities on the stress within the coal seam is small and the stress within the coal seam is basically unchanged, i.e., the original stress zone.

2 Closer to the working face, the stress within the coal seam gradually increases and the maximum stress concentration is reached 1.2 m away from the working face, i.e., the stress concentration zone.

3 Close to the working face, the stress within the coal seam gradually decreases, i.e., the stress unloading zone.

In addition, Figure 5(a) illustrates the evolution law of the stress distribution of the coal seam with time after exposure of the working face, revealing that the maximum value of the stress peak within the stress concentration zone increases from 13.1 to 13.3 and 13.5 MPa as the exposure time of the working face is extended from 20 to 50 and 100 min, respectively. In other words, the peak stress concentration within the coal seam gradually increases with prolonged exposure of the working face.

Figure 4 Evolution characteristics of each physical field during mining of a conventional coal seam (see online version for colours)

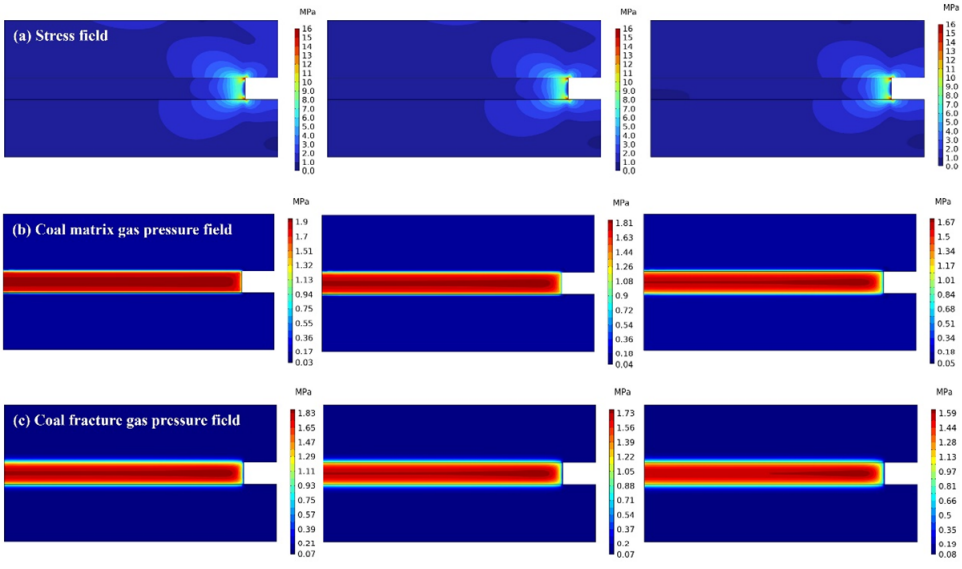

The stress state within a coal seam changes during mining, which impacts the gas distribution within the seam. Figure 4(b) and Figure 4(c) present the gas pressure change characteristics in the coal matrix and fracture during mining of a conventional coal seam. The gas pressures within the coal matrix and fracture remain basically unchanged during the initial exposure of the working face; however, the gas pressures within the coal matrix and fracture accumulate in the area close to the working face as the exposure time is extended to 120 min. Figure 5(c) and Figure 5(d) illustrate the gas pressure distribution

on the monitoring line of the coal seam, revealing that the gas pressure within the coal matrix is higher than that within the coal fracture at the same time. Taking the gas pressure change in the original rock stress area as an example, the initial gas pressure within the coal matrix is 2.0 MPa, which decreases to 1.93, 1.81, and 1.65 MPa after 20, 50, and 100 min, respectively, while the corresponding gas pressure within the coal fracture is 1.84, 1.72, and 1.56 MPa, respectively. This finding was attributed to the adsorbed gas on the coal matrix first desorbing and diffusing into the coal fracture during mining, and free gas seeping into the coal fracture and finally being discharged from the working face (Liu et al., 2022), leading to the gas pressure change in the coal fracture lagging behind that in the coal matrix. In addition, as shown in Figure 5(c) and Figure 5(d), the trend in gas pressure change within the coal seam can be divided into a slow rising stage and sharp decline stage. In the former stage, the gas pressure within the coal seam gradually increases from the original rock stress zone to the location of the peak stress but the overall change is small, only rising by 0.3 MPa on the 100th day. In the latter stage, the gas pressure within the coal seam falls drastically from the location of peak stress to the exposed working face, i.e., the stress unloading zone (Shen, 2021). In this zone, the gas pressure within the coal matrix decreases by 1.2 MPa on the 100th day, while that within the coal fracture decreases by 1.6 MPa. The increased gas pressure gradient in the stress unloading zone leads to the generation of high tensile stresses in the area close to the working face (Zhang et al., 2024a), greatly increasing the risk of the occurrence of a coal and gas outburst disaster.

Figure 5 Evolution pattern of each physical field during mining of a conventional coal seam, (a) stress field (b) permeability field (c) coal matrix gas pressure field (d) coal fracture gas pressure field (see online version for colours)

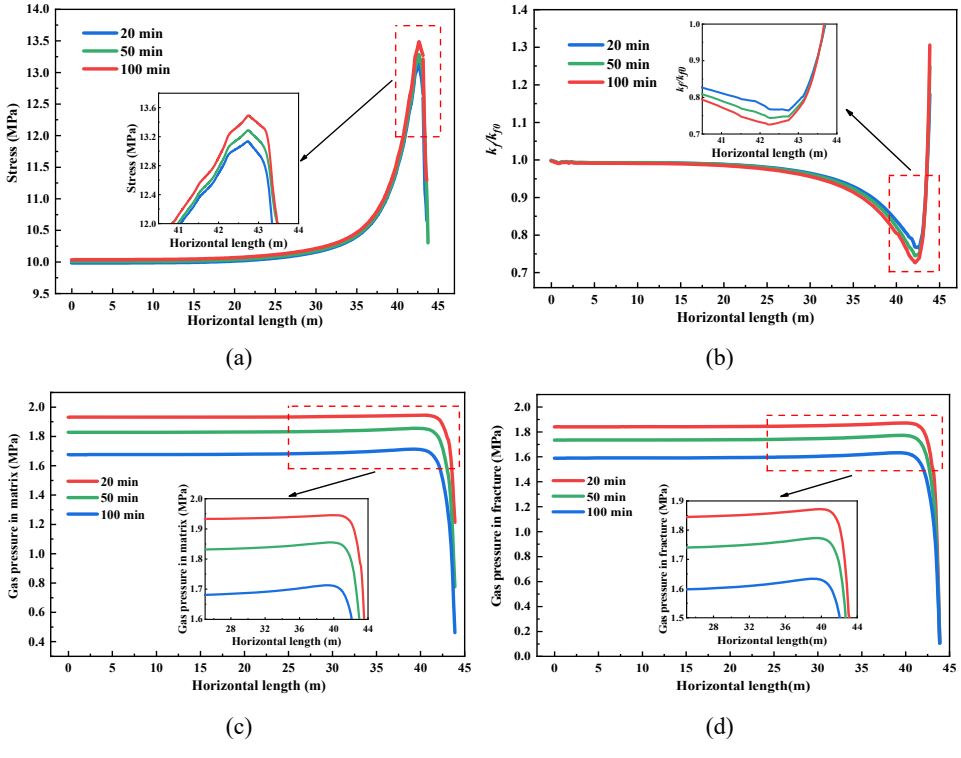

The dynamic evolution of permeability in coal seams plays a key role in the development of coal and gas outburst disasters (Zhang et al., 2024b). Therefore, this study analysed the permeability distribution characteristics of the monitoring line of the coal seam, as shown in Figure 5(b). The permeability change within the coal seam can also be divided into three zones:

1 in the original stress zone, the permeability of the coal seam basically remains unchanged

2 in the stress concentration zone, the permeability of the coal seam gradually decreases

3 the permeability of the coal seam reaches the minimum value at the location of peak stress, and then gradually increases within the stress unloading zone.

In addition, the permeability in the peak stress area of the coal seam decreases from 0.7623 to 0.7422 and 0.7240 as the exposure time of the working face is extended from 20 to 50 and 100 min, respectively. Although the discharge of coal seam gas improves the strength of the coal body (Wang et al., 2023), the stress affects the permeability of the coal seam, and the effect of mining activities on the coal seam stress increases with prolonged exposure time of the working face (Cai et al., 2019), leading to a gradual reduction in permeability within the stress concentration zone of the coal seam with extended exposure time. The reduced permeability of the coal seam hinders gas diffusion and migration within the coal matrix and fracture. Serious gas accumulation occurs within the stress concentration zone of the coal seam when the gas is not able to be discharged in a timely manner, such as in high-gas mines, ultimately leading to the occurrence of coal and gas outbursts.

Figure 6 Evolution characteristics of each physical field during mining of a fault-containing coal seam (see online version for colours)

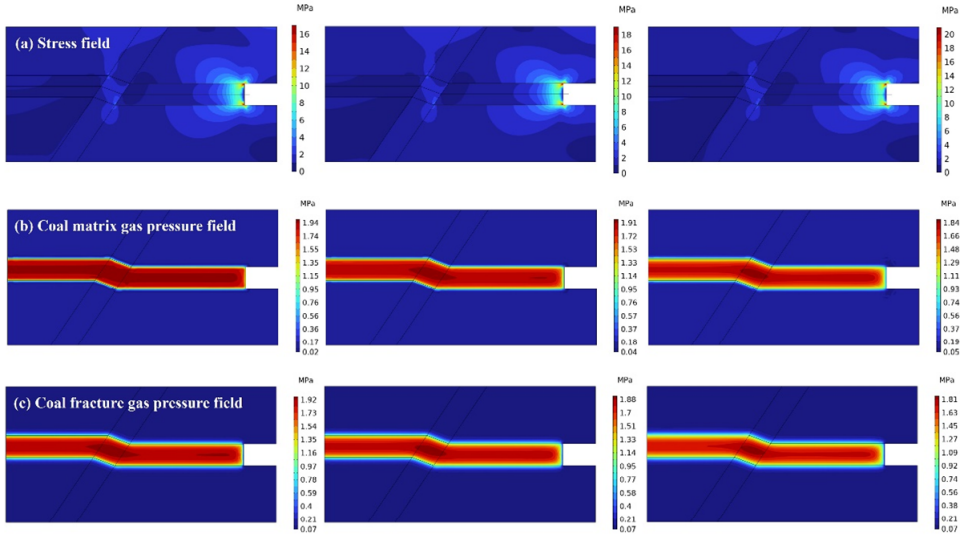

4.2 Analysis of multi-physical field coupling in fault-containing coal seams

Figure 6(a) presents the stress distribution during the mining of a fault-containing coal seam, revealing that stress concentration occurs in the area close to the working face, similar to the stress distribution during the mining of a conventional coal seam; however, there is also a high stress distribution in the fault tectonic area. To investigate the influence of faults on the stress distribution within the coal seam, the stress evolution on the monitoring line of the coal seam was analysed, as shown in Figure 7(a). In the left and right areas close to the fault tectonic area, the stress within the coal seam appears to first increase and then decrease, dropping to its lowest value at the interface between the coal seam and the fault. In addition, stress concentration appears within the fault tectonic area, which is smaller than the maximum stress concentration in the front of the working face. The peak stress in the fault stress concentration zone increases from 10.8 to 11.8 and 12.5 MPa as the exposure time of the working face is extended from 20 to 50 and 100 min, respectively, representing increases of 9.3% and 5.9%. The corresponding peak stress in the area in the front of the working face increases from 12.3 to 15.2 and 18.4 MPa, representing increases of 23.6% and 21.1%. The presence of fault tectonics leads to more significant stress changes within the coal seam than within a conventional coal seam, and the maximum stress concentration in the front of the working face of the fault-containing coal seam in the 100th min after exposure of the working face is approximately 1.35 times higher than that of the conventional coal seam, increasing the risk of a coal and gas outburst.

Figure 7(c) and Figure 7(d) present the gas pressure change characteristics during the mining of a fault-containing coal seam. Unlike in the mining of a conventional coal seam, the gas pressure in a fault-containing coal seam accumulates in the fault tectonic area. In addition, greater gas accumulation occurs in the coal matrix and fracture with prolonged exposure time of the working face. The gas pressure difference between the fault zone and original stress zone within the coal matrix increases from 0.06 to 0.10 and 0.14 MPa as the exposure time of the working face is extended from 20 to 50 and 100 min, respectively, while the corresponding gas pressure difference within the coal fracture increases from 0.06 to 0.10 and 0.14 MPa.

Figure 7(b) illustrates the permeability evolution characteristics of the monitoring line during mining of the fault-containing coal seam. Owing to the effect of stress concentration, low permeability occurs in the fault tectonic area and front of the working face. The weaker mechanical strength of the coal body in the fault tectonic area leads to more greatly reduced permeability in this area. In addition, the permeability reduction in the fault tectonic area and front of the working faces increases with prolonged extension of the exposure time. The permeability of the fault tectonic area decreases from 0.6263 to 0.6125 and 0.5947 as the exposure time of the working face is extended from 20 to 50 and 100 min, respectively, and the corresponding permeability of the front of the working face decreases from 0.7310 to 0.7061 and 0.6714. The reduced permeability of the fault tectonic area and front of the working face further restricts gas migration and diffusion within the coal seam, resulting in the accumulation of gas pressure within the coal seam from the fault zone onward.

Comparing the multi-physical field evolution characteristics of the conventional coal and fault-containing coal seams reveals that the stress distribution within the coal seam is more complex and variable when mining a fault-containing coal seam. Stress concentration in the fault tectonic area leads to a reduction in permeability and limits gas

transport and diffusion within the coal seam, resulting in a substantial gas accumulation in fault-containing areas. As a result, the risk of coal and gas outbursts is higher when mining fault-containing coal seams than when mining conventional coal seams.

Figure 7 Evolution pattern of each physical field during mining of a fault-containing coal seam, (a) stress field (b) permeability field (c) coal matrix gas pressure field (d) coal fracture gas pressure field (see online version for colours)

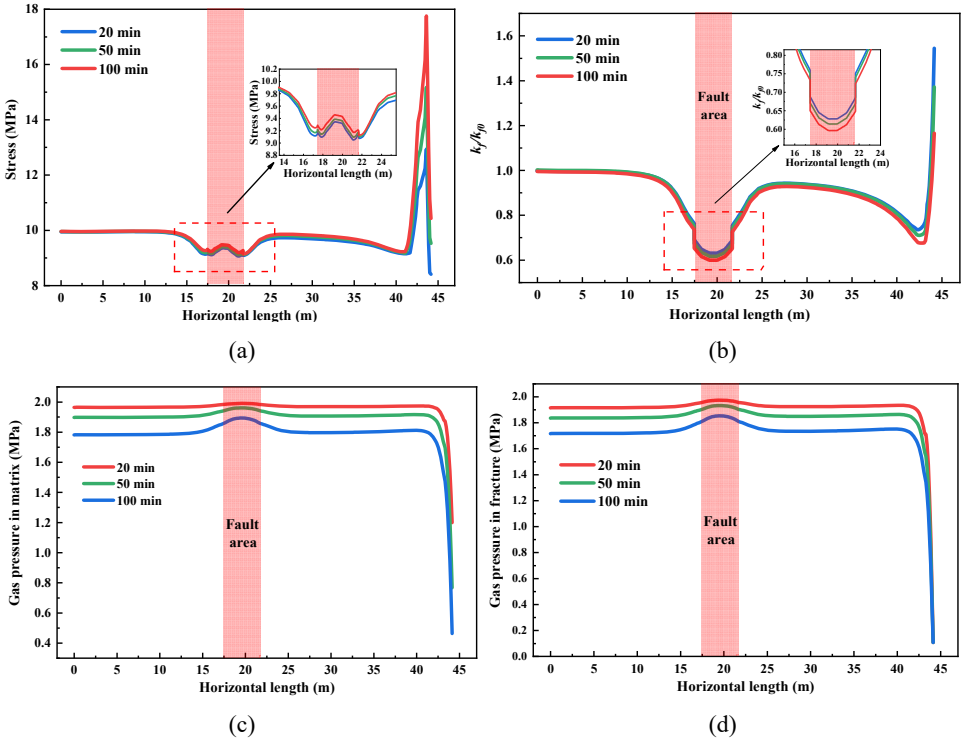

4.3 *Analysis of multi-physical field coupling in fault zones during coal seam mining*

To further analyse the influence of the mining process on the development of coal and gas outbursts when mining fault-containing coal seams, the multi-physical field coupling of the coal seam mining at 6, 12, 18 and 24 m was analysed. Figure 8(a) presents the stress distribution within the coal seam when the working face is mined to different distance. Overall, the stress distribution within the coal seam exhibits stress peaks in the fault tectonic area and near the working face, which appear to increase as the working face approaches the fault region. The peak stress within the fault tectonic area increases from 10.8 to 11.4 and 14.7 MPa when the working face advances from 6 to 12, 18, and 24 m, while the corresponding peak stress within the coal seam near the working face increases from 12.3 to 20.0 and 33.6 MPa. The peak stresses in the fault tectonic area and front of the working face are superimposed when the working face is drilled to 24 m, resulting in a sharp increase in the peak stress to 53.5 MPa. The peak stress within the coal seam increases exponentially as the working face gradually approaches the fault

tectonic area. Therefore, the front of the working face must be fully depressurised or mining should be terminated close to the fault tectonic area to ensure safety during coal mining.

Figure 8(c) and Figure 8(d) illustrate the gas distribution within the coal matrix and fracture when the coal seam is mined to different depths. The gas within the coal matrix and fracture accumulates in the fault tectonic area and front of the working face. Gas pressure accumulation within the coal seam becomes increasingly serious as the working face gradually approaches the fault tectonic area. The gas pressure difference in front of the working face increases from 0.059 to 0.093, 0.142 and 0.210 MPa as the mining distance of the working face increases from 6 to 12, 18, and 24 m, respectively.

Figure 8 Evolution pattern of each physical field during mining of a fault-containing coal seam, (a) stress field (b) permeability field (c) coal matrix gas pressure field (d) coal fracture gas pressure field (see online version for colours)

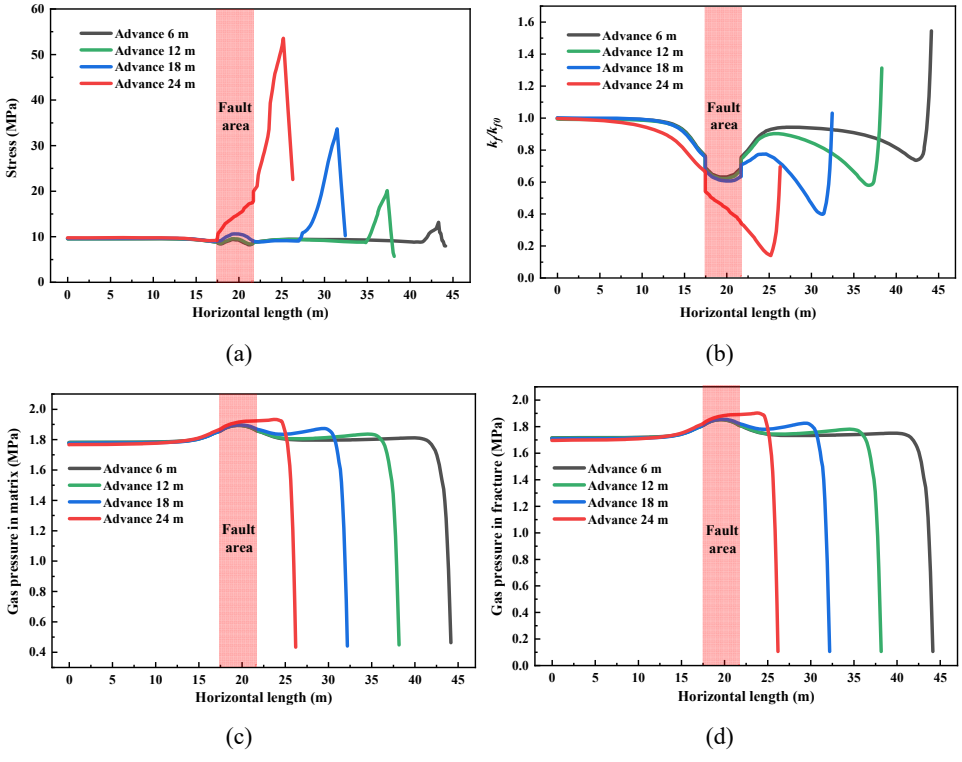

In addition, the permeability evolution of the coal seam during the mining process was analysed, as shown in Figure 8(b). Owing to the influence of stress concentration in the coal seam, the permeability of the coal seam in the fault tectonic area and front of the working face appears to decrease. The reduction in permeability becomes more serious as the working faces approach the fault tectonic area. The permeability of the fault tectonic area decreases from 0.6263 to 0.6171 and 0.6010 as the working face advances from 6 to 12 and 18 m, respectively, and the corresponding permeability close to the working face decreases from 0.7310 to 0.5752 and 0.3927. The permeability of the coal seam decreases to 0.1339 when the coal seam is mined to 24 m owing to the superimposition of stress

concentrations in the fault tectonic area and area close to the working face, which is approximately 65.9% lower than when the working face is mined to 18 m. The above analysis demonstrates that the reduction in permeability becomes more significant as the working face approaches the fault tectonic area. The reduced permeability of the coal seam further impedes gas transport and diffusion within the coal matrix and fracture, leading to the occurrence of a coal and gas outburst accident if the accumulated gas cannot be discharged in a timely manner.

4.4 Damage evolution during mining of fault-bearing coal seams

The damage area in the process of fault-containing coal seam mining was analysed using damage theory, as shown in Figure 9. It can be seen that the damage area of the coal seam will gradually become larger as the working face keeps moving forward. When the mining distance is 6 and 12 m, the top and bottom of the front of the working face and the inside of the fault only have a very small area of damage, and by integrating the damage area, it can be concluded that the damage area of the mining distance of 6 and 12 m is only 1.6 and 2.3 m^2. When the mining distance is 18 m, the damage area at the top and bottom of the front of the working face appears to be connected, and the damage area is gradually enlarged, and the total damage area is 3.6 m^2. And when the mining distance is 24 m, a large damage area of different degrees starts to appear in front of the working face and inside the fault, and the damage area reaches 15.7 m^2. It can be found that the damage area from 18 m to 24 m has a sharp trend. According to the results of the multi-physical field coupling analysis, when the mining depth of the coal seam increases from 18 m to 24 m, the coal seam stress field and the gas pressure field show a significant jump, and the coupling effect will drive the rapid expansion of the damage zone of the coal body, resulting in a nonlinear increase in the area of the damage, which will significantly exacerbate the risk of the dynamic disaster of the coal and gas outburst.

Figure 9 Damage situation of coal seams under different mining distance (see online version for colours)

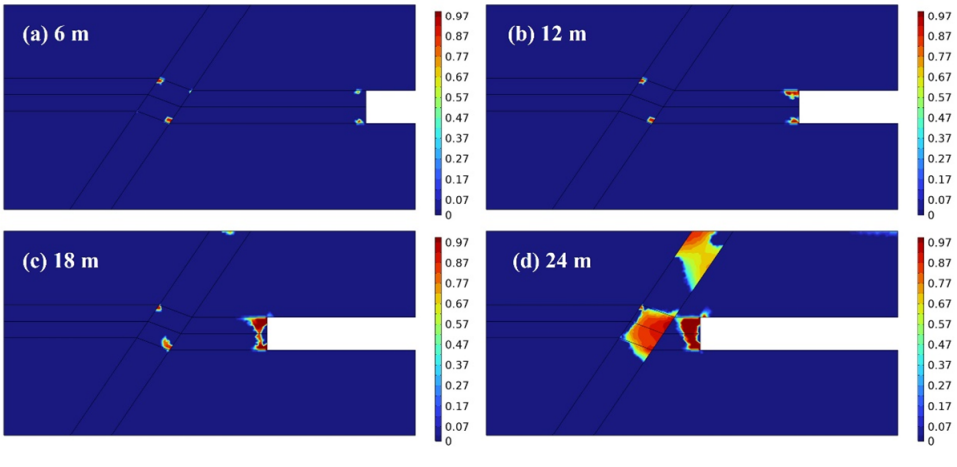

4.5 Energy evolution of coal seam mining near fault zones

4.5.1 Energy theory of coal and gas outburst

The energy theory is often used to quantitatively describe and explain some of the physical phenomena during gas outburst. Coal and gas outburst disasters occur as a result of the combined effects of stress, gas and coal strength. Previous studies have shown that during gas outburst, the coal elastic energy and gas expansion energy are converted into the crushing work of the coal, the throwing work of the broken coal, and other dissipated energies. In the gestation stage of gas outburst, the coal elastic energy and gas expansion energy dominate the gas outburst process.

1 Elastic energy of coal

Influenced by the ground stress, the deformation of coal in compression state is in accordance with Hooke's law. Under triaxial stress state, the elastic energy per unit volume of coal is proportional to the stress in three directions, but inversely proportional to the elastic modulus of coal. Therefore, the elastic energy per unit volume of coal can be expressed as:

$$E_e = \frac{{\sigma_1}^2 + {\sigma_2}^2 + {\sigma_3}^2 - 2v\left(\sigma_1\sigma_2 + \sigma_2\sigma_3 + \sigma_3\sigma_1\right)}{2E} \tag{14}$$

where E_e is the modulus of elasticity of the coal; σ_1, σ_2 and σ_3 are the three directions stresses of the coal.

2 Gas expansion energy

Based on the dual porosity characteristics of the coal, the gas inside the coal can be divided into adsorbed gas and free gas. Therefore, the gas expansion energy can also be divided into adsorbed gas expansion energy and free gas expansion energy. The gas expansion energy per unit mass of coal can be expressed as:

$$E_{\mathrm{g}} = \frac{p_{\mathrm{atm}} V_0}{n-1}\left[\left(\frac{p}{p_{\mathrm{atm}}}\right)^{\frac{n-1}{n}} - 1\right] \tag{15}$$

where E_g is the expansion energy of gas per unit mass of coal, p_{atm} is the pressure in the roadway, and the value here is 0.1 MPa, n is the multivariate process parameter, n is 1~1.31, and the value here is 1.25, and V_0 is the volume of adsorbed gas participating in the protrusion process.

Coal and gas outburst is viewed as a multivariate process in the study (Lu et al., 2019), so the following relationships exist:

$$p_{atm}{V_{f0}}^n = p_f {V_f}^n \tag{16}$$

Substituting the above equation into equation (15), the free gas expansion energy per unit volume of coal can be expressed as:

$$E_{\mathrm{g}}^{free} = \rho_c \frac{p_{\mathrm{atm}} V_{f0}}{n-1}\left[\left(\frac{p_f}{p_{\mathrm{atm}}}\right)^{\frac{n-1}{n}} - 1\right] \tag{17}$$

Coal and gas outburst is an extremely complex process, and the adsorbed gas volume involved during gas outburst is difficult to be calculated. According to the results of previous laboratory research (Wang et al., 2023b), the gas desorption volume of coal in a short time can be expressed as:

$$\frac{V_t}{V_\infty} = \frac{6}{\sqrt{\pi}} \frac{\sqrt{D}}{r} \sqrt{t} = 6\sqrt{\frac{D_e}{\pi}\sqrt{t}} \tag{18}$$

where r is the radius of the broken coal, and t is the desorption time.

The limiting gas desorption of a coal can be expressed as:

$$V_\infty = \frac{abp_m}{1+bp_m} - \frac{abp_{atm}}{1+bp_{atm}} \tag{19}$$

The adsorbed gas expansion energy per unit volume of coal is obtained by substituting equations (18) and (19) into equation (15):

$$E_{\mathrm{g}}^{ads} = \rho_c \frac{p_{atm}}{n-1}\left(6\sqrt{\frac{D_e}{\pi}\sqrt{t}}\right)\left(\frac{abp_m}{1+bp_m} - \frac{abp_{atm}}{1+bp_{atm}}\right)\left[\left(\frac{p}{p_{atm}}\right)^{\frac{n-1}{n}} - 1\right] \tag{20}$$

3 Crushing energy

The surface area of a coal body increases after damage and destruction, and the energy done to produce the new surface area is called crushing energy. The crushing energy of coal body can be expressed as (Lu et al., 2022):

$$E_b = s_b w_b \rho_b \tag{21}$$

where s_b is the new specific surface area of the crushed coal body, cm^2/g, the new specific surface area is usually located in 113~525 cm^2/g, take 120 cm^2/g; *wb* is the specific energy of the coal crushing, MJ/cm^2, $w_b = 10.43 \times 10^{-3}$ f; f is the coefficient of firmness.

4 Gas outburst criterion

In this study, the ratio of gas outburst potential and dissipation energy (crushing energy) of the coal body in the damage area is defined as the gas outburst criterion. When the ratio is less than 1, it indicates that the coal seam has no danger of gas outburst; when the ratio den equals to 1, it indicates that the coal seam is in the critical state of gas outburst; when the ratio is greater than 1, it indicates that the coal seam has the danger of gas outburst. And the larger the value is, the higher the danger of gas outburst is. The gas outburst criterion of coal body can be expressed as:

$$C = \frac{\int_{Vp}\left(E_e + E_g^{fre} + E_g^{ads}\right)dV}{\int_{Vp} E_b dV} \tag{22}$$

where V_p is the area of coal seam damage destruction area, m^3.

4.5.2 Energy evolution law during coal seam mining near faults

Figure 10 shows the energy evolution process during the fault-containing coal seam excavation. It can be seen that as the working face gradually approaches the fault structure area, the gas outburst energy per unit volume of coal seam shows an upward trend, and the elastic energy and gas expansion energy of the coal body are the important components of the gas outburst energy (Cheng et al., 2023). As the working face gradually approaches the fault area, the elastic energy per unit volume of coal body in front of the mining work is gradually increasing. When the coal seam is mined for 6, 12, 18 and 24 m, the elastic energy of the unit volume of coal in front of the working face is 0.06, 0.07, 0.08 and 0.09 MJ/m^3, respectively. The elastic energy within the coal seam is mainly released outward in the form of deforming the coal (Cheng and Wang, 2024), and compression deformation of the coal seam leads to the reduction of its permeability, which in turn raises the gas expansion energy within the coal seam. It can be seen in Fig. 10 that as the working face gradually approaches the fault area, both the adsorbed gas expansion energy and the free gas expansion energy within the coal seam also show a rising trend. The adsorbed gas expansion energy per unit volume of coal in front of the working face was 0.17, 0.19, 0.26 and 0.34 MJ/m^3, while the free gas expansion energy was 0.05, 0.06, 0.09 and 0.11 MJ/m^3, when the coal seam was mined for 6, 12, 18 and 24 m. Compared with the adsorbed gas expansion energy, the free gas expansion energy accounted for a small portion of the total gas outburst energy, and the maximum is only 21%.

Figure 10 Energy evolution during mining of fault- containing coal seam (see online version for colours)

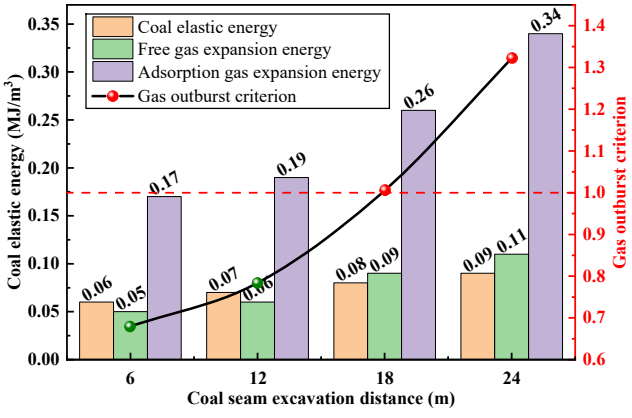

Figure 10 also shows the results of the gas outburst criterion based on the energy theory, when the coal seam is mined for 6 and 12 m, the gas outburst criterion of the coal seam is less than 1. Although there is a small damage area in the coal seam (Figure 1), but at this time, the coal seam does not have a gas outburst danger. When the coal seam continues to be mined to 18 m, the gas outburst criterion of the coal seam in front of the mining work is 1.02, which just exceeds the critical value of coal seam gas outburst, and at this time, the coal seam has a certain risk of gas outburst, which will result in accidents if gas outburst prevention and control measures are not taken in time or mining is stopped. According to the simulation results, when the coal seam continues to be mined to 24 m,

the gas outburst criterion of the coal seam reaches 1.32, and at this time, a large range of damage occurs in front of the working face and in the area of the fault [Figure 9(d)].

Based on the above analysis, it can be concluded that under the influence of mining disturbance, the migration sequence of gas within the coal seam is: adsorbed gas on the coal matrix-free gas inside the coal fracture - external environment. Although the free gas inside the coal fracture is in direct contact with the external environment, it does not lead to gas outburst due to the relatively low percentage of free gas expansion energy in the total energy of gas outburst. The key to the initiation of gas outburst lies in the instantaneous massive release of adsorbed gas energy (Qin et al., 2024). As the working face gradually approaches the fault area, the higher the elastic energy contained in the tectonic coal under the same stress environment due to the lower strength of the tectonic coal. The coal seam needs to produce greater deformation to release the high elastic energy, which leads to a further reduction in the permeability of the coal seam. In addition, the presence of tectonic coals accelerates the rate of gas desorption from primary coal in the surrounding area, which makes it easier for the accumulated gas expansion energy to reach the gas outburst threshold, thus increasing the risk of coal and gas outburst. Therefore, the focus of measures to prevent and control the risk of gas outburst should focus on reducing the high elastic energy formed by the stresses in the coal seam, as well as the high gas expansion energy formed by the accumulation of gas.

5 Conclusions

1 Compared with conventional coal seam mining, during the mining process of fault-containing coal seam, stress concentration occurs both in the fault area and in front of the exposed working face, which further compresses the coal seam and causes its permeability to drop to 1/7 of the initial permeability, and results in gas accumulation both in the fault area and in front of the exposed working face. And the longer the exposure time of the working face, the more severe the gas accumulation phenomenon.

2 Coal elastic energy and adsorbed gas expansion energy dominate the evolution process of gas outburst gestation stage. The mining activity increases the elastic energy of the coal body in front of the working face, and the elastic energy is mainly released to the outside through the deformation of the coal body. However, the compression deformation of the coal body will hinder the migration of gas, resulting in the increase of gas expansion energy in the coal body. Since the free gas expansion energy accounts for a relatively low percentage in the total gas outburst energy (up to 21% only). The key to the initiation of gas outburst lies in the instantaneous massive release of adsorbed gas energy.

3 As coal seam mining continues to approach the fault area, the damage area of the coal seam due to the coupling effect of multiple physical fields increases exponentially, and the risk of coal and gas outburst also rises gradually. In order to ensure the safe mining of coal seams, the hidden structures in the coal seams should be detected in advance, and the stress in the coal seams in the tectonic area should be fully unloaded, and the extraction intensity of the coal seam gas should be increased.

So as to prevent and control the occurrence of coal and gas dynamic disaster from multiple angles.

Declarations

The authors declare they have no potential conflicts of interest with respect to the research, authorship, and/or publication of this article.

Data availability

Enquiries about data availability should be directed to the authors.

References

Cai, W., Dou, L., Wang, G. et al. (2019) 'Mechanism of fault reactivation and its induced coal burst caused by coal mining activities', *Journal of Mining & Safety Engineering*, Vol. 36, No. 6, pp.1193–1202, DOI: 10.13545/j.cnki.jmse.2019.06.016.

Cao, J. (2024) 'Analysis of the statistical laws and dynamic effect characteristics of coal and gas outburst accidents in China in recent 10 years', *Mining Safety & Environmental Protection* Vol. 51, No. 3, pp.36–42+49, DOI: 10.19835/j.issn.1008-4495.20240446.

Cao, Y., Zhang, H., Zhang, Z. et al. (2022) 'Characteristics of coal and gas outburst and controlling mechanism of stress field in the hanging wall of normal faults', *Coal Geology & Exploration* Vol. 52, No. 4, pp.61–69, DOI: 10.12363/issn.1001-1986.21.08.0420.

Chen, X., Li, L., Yuan, Y. et al. (2019) 'Effect and mechanism of geological structures on coal seam gas occurrence in Changping minefield', *Energy Science & Engineering* Vol. 8, No. 1, pp.104–115, https://doi.org/10.1002/ese3.512.

Cheng, Y. and Lei, Y. (2021) 'Causality between tectonic coal and coal and gas outbursts', *Journal of China Coal Society* Vol. 46, No. 1, pp.180–198, DOI: 10.13225/j.cnki.jccs.YG20.1539.

Cheng, Y. and Wang, C. (2024) 'Deformation energy of tectonic coal and its role in coal and gas outbursts', *Journal of China Coal Society*, Vol. 49, No. 2, pp.645–663, DOI: 10.13225/j.cnki.jccs.2023.0884.

Cheng, Y., Lei, Y. and Yang, S. (2023) 'Energy principle of simulation experiments on coal and gas outburst', *Journal of China Coal Society* Vol. 48, No. 11, pp.4078–4096, DOI: 10.13225/j.cnki.jccs.2023.0813.

Fan, C., Li, S., Luo, M. et al. (2017) 'Coal and gas outburst dynamic system', *International Journal of Mining Science and Technology*, Vol. 27, No. 1, pp.49–55, https://doi.org/10.1016/j.ijmst.2016.11.003.

Fan, C., Zhang, X., Yang, L. et al. (2024) 'Spatial and temporal distribution of coal and gas outburst accidents in China from 1950 to 2022', *Journal of Liaoning Technical University (Natural Science)*, Vol. 43, No. 3, pp.279–287, https://doi:10.11956/j.issn.1008-0562.20230235.

Fu, J., Li, B., Ren, C. et al. (2022) 'Coupling between damage evolution and permeability model with the adsorption effect for coal under gas extraction and coal mining conditions', *Energy & Fuels*, Vol. 36, No. 18, pp.10813–10831, https://doi.org/10.1021/acs.energyfuels.2c01758.

Gao, K., Huang, P., Liu, Z. et al. (2021) 'Coal-rock damage characteristics caused by blasting within a reverse fault and its resultant effects on coal and gas outburst', *Scientific Reports*, Vol. 11, p.19158, https://doi.org/10.1038/s41598-021-98581-w.

Guo, D., Chuai, X., Zhang, J. et al. (2023) 'Controlling effect of tectonic stress field on coal and gas outburst', *Journal of China Coal Society* Vol. 48, No. 8, pp.3076–3090, DOI: 10.13225/j.cnki.jccs.2022.1435.

Jia, J., Jia, Q., Sang, X. et al. (2023) 'Review and prospect of coal mine geological guarantee system in China during 30 years of construction', *Coal Geology & Exploration*, Vol. 51, No. 1, pp.86–106, DOI: 10.12363/issn.1001-1986.22.07.0564.

Li, P. and Zhang, X. (2022) 'Analysis of gas migration law in coal seam in structural zone', *Coal Science & Technology Mazazine*, Vol. 50, No. 10, pp.93–101, DOI: 10.13199/j.cnki.cst.2021-0323.

Li, Z., Yu, H., Bai, Y. et al. (2023) 'Numerical study on the influence of temperature on CO2-ECBM', *Fuel*, Vol. 348, p.128613, https://doi.org/10.1016/j.fuel.2023.128613.

Liu, J., Zhai, Y., Zhang, H. et al. (2024a) 'Mechanical damage characteristics of structural coal particles under uniaxial loading and unloading', *Coal Science & Technology Mazazine*, Vol. 45, No. 4, pp.85–90, DOI: 10.19896/j.cnki.mtkj.2024.04.016.

Liu, W., Han, D., Guo, M. et al. (2024b) 'Evaluation of adsorbed and free gas in the coal matrix during desorption processes: insights from experimental and numerical methods', *Fuel*, Vol. 376, p.132739, https://doi.org/10.1016/j.fuel.2024.132739.

Liu, Q., Cheng, Y., Haifeng, W. et al. (2015) 'Numerical assessment of the effect of equilibration time on coal permeability evolution characteristics', *Fuel*, Vol. 140, pp.81–89, https://doi.org/10.1016/j.fuel.2014.09.099.

Liu, Q., Chu, P., Huang, W. et al. (2022) 'Gas desorption diffusion hysteresis pressure and the matrix fracture mass transfer function of dual porosity coal', *Journal of China Coal Society* Vol. 47, No. 2, pp.870–882, DOI: 10.13225/j.cnki.jccs.XR21.1351.

Liu, T., Lin, B., Yang, W. et al. (2017) 'Coal permeability evolution and gas migration under non-equilibrium state', *Transport in Porous Media*, Vol. 118, No. 3, pp.393–416, https://doi.org/10.1007/s11242-017-0862-8.

Lu, S., Li, M., Si, S. et al. (2022) 'Analysis of outburst instability tendency of coal containing methane based on energy theory', *Safety in Coal Mines*, Vol. 53, No. 10, pp.105–111, DOI: 10.13347/j.cnki.mkaq.2022.10.014.

Lu, S., Zhang, Y., Sa, Z. et al. (2019) 'Criterion of plastic failure and outburst energy instability of soft and hard composite coal', *Journal of Mining & Safety Engineering*, Vol. 36, No. 3, pp.583–592, DOI: 10.13545/j.cnki.jmse.2019.03.020.

Luo, J., Li, Y., Meng, X. et al. (2023) 'Influence of coupling mechanism of loose layer and fault on multi-physical fields in mining areas', *International Journal of Coal Science & Technology* Vol. 10, p.86, https://doi.org/10.1007/s40789-023-00640-2.

Meng, Z., Zhang, K. and Shen, Z. (2022) 'Difference analysis of methane diffusion properties between tectonic coal and primary coal', *Coal Geology & Exploration*, Vol. 50, No. 3, pp.102–109, DOI: 12363/issn.1001-1986.21.12.0799.

Mora, C.A. and Wattenbarger, R.A. (2009) 'Analysis and verification of dual porosity and CBM shape factors', *Journal of Canadian Petroleum Technology*, Vol. 48, No. 2, pp.17–21, https://doi.org/10.2118/09-02-17.

Peng, R., Xue, D., Sun, H. et al. (2019) 'Characteristics of strong disturbance to rock mass in deep mining', *Journal of China Coal Society*, Vol. 44, No. 5, pp.1359–1368, DOI: 10.13225/j.cnki.jccs.2019.6024.

Qin, Y., Su, W., Lu, S. et al. (2024) 'Research on energy instability of composite coal based on unsteady diffusion to cause disaster', *Coal Science and Technology*, Vol. 52, No. 7, pp.126–138, DOI: 10.12438/cst.2023-0984.

Qu, H., Peng, Y., Liu, J. et al. (2018) 'Impact of gas adsorption on apparent permeability of shale fracture and shale gas recovery rate', *Scientia Sinica Technologica*, Vol. 48, No. 8, pp.891–900, https://doi.org/10.1360/N092017-00196.

Shen, Z. (2021) 'Reasonable position of pressure relief roadway in high stress area and test analysis of pressure relief effect', *Hans Journal of Civil Engineering*, Vol. 10, No. 3, pp.195–201, https://doi.org/10.12677/hjce.2021.103022.

Song, Z. and Wei, G. (2017) 'Control effect of small faults on coal and gas outburst in Xuehu mine', *Safety in Coal Mines*, Vol. 48, No. 12, pp.153–156, DOI: 10.13347/j.cnki.mkaq.2017.12.041.

Wang, C., Liu, L., Li, X. et al. (2023a) 'Mechanism of gas pressure action during the initial failure of coal containing gas and its application for an outburst inoculation', *International Journal of Mining Science and Technology*, Vol. 33, No. 12, pp.1511–1525, https://doi.org/10.1016/j.ijmst.2023.11.001.

Wang, D., Pang, X., Wei, J. et al. (2023b) 'Effect of gas properties and pore pressure on the microcrack propagation in coal', *Coal Science and Technology*, Vol. 51, No. 2, pp.183–192, DOI: 10.13199/j.cnki.cst.2022-1417.

Wang, Z. and Cheng, Y. (2017) 'Experiment on pore characteristics and gas desorption law of structural coal and primary structure coal', *Coal Science and Technology*, Vol. 45, No. 3, pp.84–88, DOI: 10.13199/j.cnki.cst.2017.03.015.

Xie, H., Zhang, R., Zhang, Z. et al. (2023) 'Reflections and explorations on deep earth science and deep earth engineering technology', *Journal of China Coal Society*, Vol. 48, No. 11, pp.3959–3978 [online] https://link.cnki.net/doi/10.13225/j.cnki.jccs.2023.0989.

Zhang, C., Liu, M., Wang, E. et al. (2024a) 'Influence law and control mechanism of coal seam permeability on coal and gas outburst', *Journal of China Coal Society*, Vol. 49, No. 12, pp.4842–4854, DOI: 10.13225/j.cnki.jccs.2024.0382.

Zhang, S., Cui, J. and He, S. (2024b) 'Coupling mechanism of seepage and coal and rock mass destruction during coal and gas outburst', *Coal Science and Technology*, Vol. 52, No. 12, pp.105–115, DOI: 10.12438/cst.2023-1573.

Zhang, H., Liu, J. and Elsworth, D. (2008) 'How sorption-induced matrix deformation affects gas flow in coal seams: a new FE model', *International Journal of Rock Mechanics and Mining Sciences*, Vol. 45, No. 8, pp.1226–1236, https://doi.org/10.1016/j.ijrmms.2007.11.007Get rights and content.

Zhao, Y. (2021) 'Retrospection on the development of rock mass mechanics and the summary of some unsolved centennial problems', *Chinese Journal of Rock Mechanics and Engineering* Vol. 40, No. 7, pp.1297–1336, DOI: 10.13722/j.cnki.jrme.2021.0617.

Zhao, Y., Lin, B., Liu, T. et al. (2019) 'Flow field evolution during gas depletion considering creep deformation', *Journal of Natural Gas Science and Engineering*, Vol. 65, pp.45–55, https://doi.org/10.1016/j.jngse.2019.02.008.

Zhao, Y., Lin, B., Liu, T. et al. (2020) 'Mechanism of multifield coupling-induced outburst in mining-disturbed coal seam', *Fuel*, Vol. 272, p.117716, https://doi.org/10.1016/j.fuel.2020.117716.

Zheng, C., Kizil, M.S., Aminossadati, S.M. et al. (2018a) 'Effects of geomechanical properties of interburden on the damage-based permeability variation in the underlying coal seam', *Journal of Natural Gas Science and Engineering*, Vol. 55, pp.42–51, https://doi.org/10.1016/j.jngse.2018.04.017.

Zheng, C., Kizil, M.S., Chen, Z. et al. (2018b) 'Role of multi-seam interaction on gas drainage engineering design for mining safety and environmental benefits: linking coal damage to permeability variation', *Process Safety and Environmental Protection*, Vol. 114, pp.310–322, https://doi.org/10.1016/j.psep.2018.01.011.